HHS Public Access

Author manuscript

J Expo Sci Environ Epidemiol. Author manuscript; available in PMC 2024 June 19.

Published in final edited form as:

J Expo Sci Environ Epidemiol. 2023 July ; 33(4): 537–547. doi:10.1038/s41370-023-00577-3.

Effects of Corsi-Rosenthal boxes on indoor air contaminants: non-targeted analysis using high resolution mass spectrometry

Katherine E. Manz[1,✉], **Robin E. Dodson**[2], **Yun Liu**[3], **Lukas Scheidl**[1], **Shaunessey Burks**[3], **Fiona Dunn**[1], **Richa Gairola**[3], **Nina Franzen Lee**[3], **Erica D. Walker**[3], **Kurt D. Pennell**[1], **Joseph M. Braun**[3,✉]

[1]School of Engineering, Brown University, Providence, RI 02912, USA.

[2]Silent Spring Institute, Newton, MA 02460, USA.

[3]Department of Epidemiology, Brown University, Providence, RI 02912, USA.

Abstract

BACKGROUND: In response to COVID-19, attention was drawn to indoor air quality and interventions to mitigate airborne COVID-19 transmission. Of developed interventions, Corsi-Rosenthal (CR) boxes, a do-it-yourself indoor air filter, may have potential co-benefits of reducing indoor air contaminant levels.

OBJECTIVE: We employed non-targeted and suspect screening analysis (NTA and SSA) to detect and identify volatile and semi-volatile organic contaminants (VOCs and SVOCs) that decreased in indoor air following installation of CR boxes.

METHODS: Using a natural experiment, we sampled indoor air before and during installation of CR boxes in 17 rooms inside an occupied office building. We measured VOCs and SVOCs using gas chromatography (GC) high resolution mass spectrometry (HRMS) with electron ionization (EI) and liquid chromatography (LC) HRMS in negative and positive electrospray ionization (ESI). We examined area count changes during vs. before operation of the CR boxes using linear mixed models.

✉**Correspondence** and requests for materials should be addressed to Katherine E. Manz or Joseph M. Braun. katherine_manz@brown.edu; joseph_braun_1@brown.edu.

AUTHOR CONTRIBUTIONS

KEM—Conceptualization, Methodology, Validation, Formal analysis, Writing - Original Draft, Writing - Review & Editing, Visualization, Supervision; RED—Conceptualization, Methodology, Writing - Original Draft, Writing - Review & Editing, Visualization, Supervision, Project Administration; YL—Formal analysis, Writing - Original Draft, Writing - Review & Editing; LS—Methodology, Validation, Data Curation, Formal analysis, Writing - Original Draft, Writing - Review & Editing; SB—Methodology, Writing - Original Draft, Writing - Review & Editing; FD—Methodology, Formal analysis, Writing - Original Draft, Writing - Review & Editing; RG—Formal analysis, Writing - Original Draft, Writing - Review & Editing; NFL—Methodology, Writing - Original Draft, Writing - Review & Editing; EDW—Methodology, Writing - Original Draft, Writing - Review & Editing; KDP—Methodology, Writing - Original Draft, Writing - Review & Editing; JMB—Conceptualization, Methodology, Validation, Formal analysis, Writing - Original Draft, Writing - Review & Editing, Visualization, Supervision, Project administration, Funding acquisition.

COMPETING INTERESTS

JB was financially compensated for his services as an expert witness for plaintiffs in litigation related to PFAS-contaminated drinking water.

Supplementary information The online version contains supplementary material available at https://doi.org/10.1038/s41370-023-00577-3.

RESULTS: Transformed (log2) area counts of 71 features significantly decreased by 50–100% after CR boxes were installed (False Discovery Rate (FDR) p-value < 0.2). Of the significantly decreased features, four chemicals were identified with Level 1 confidence, 45 were putatively identified with Level 2–4 confidence, and 22 could not be identified (Level 5). Identified and putatively identified features (Level ≥4) that declined included disinfectants (n = 1), fragrance and/or food chemicals (n = 9), nitrogen-containing heterocyclic compounds (n = 4), organophosphate esters (n = 1), polycyclic aromatic hydrocarbons (n = 8), polychlorinated biphenyls (n = 1), pesticides/herbicides/insecticides (n = 18), per- and polyfluorinated alkyl substances (n = 2), phthalates (n = 3), and plasticizers (n = 2).

Keywords

Non-targeted analysis (NTA); Exposome; Air quality; Interventions; Corsi-Rosenthal (CR) boxes; High resolution mass spectrometry

INTRODUCTION

Humans spend a large fraction of time indoors. Often, pollutant levels indoors are higher relative to outdoors. Therefore, indoor air pollutants are an important component of the human exposome [1], which is defined as the totality of exposures throughout an individual's life [2]. The indoor air exposome is comprised of known constituents such as particulate matter (PM), volatile organic contaminants (VOCs), and semi-volatile organic contaminants (SVOCs), which have been linked to adverse health effects including allergies, cancer, endocrine disruption, and pre-mature mortality [1, 3, 4]. Sources of chemical emissions in the indoor environment include migration of outdoor air, migration of gas from soil or groundwater, and off gassing from furniture, carpeting, electronics, decorations, and consumer products [5–7].

Recently, we took advantage of a natural experiment to examine changes in per- and polyfluoalkyl substances (PFAS) and other SVOCs in indoor air using Corsi-Rosenthal (CR) boxes [8]. The CR box is a "do-it-yourself" air filter consisting of four consumer-grade MERV-13 (or equivalent) filters and a box fan that was designed in response to the COVID-19 pandemic to reduce levels of airborne viral particles from indoor environments [9]. We used targeted mass spectrometry to quantify air concentrations of 42 PFAS and 24 other SVOCs, including phthalates, organophosphate esters (OPEs), polychlorinated biphenyls (PCBs), and brominated flame retardants (BDEs) [8]. We found that CR boxes reduced air concentrations of seven PFAS (N-ethyl perfluorooctanesulfonamidoethanol, N-ethyl perfluorooctanesulfonamide, perfluorobutane sulfonamide, perfluorobutanesulfonic acid, perfluorohexanesulfonic acid, perfluorooctanesulfonic acid, and perfluorononanoic acid) and five phthalates (dimethyl phthalate, diethyl phthalate, diisobutyl phthalate, butyl benzyl phthalate, and dicyclohexyl phthalate) [8]. However, CR boxes may remove other potentially toxic contaminants from indoor air that were not assessed using targeted analytical methods. Therefore, non-targeted analysis (NTA) and suspect screening analysis (SSA) may help to characterize the ability of CR boxes to improve the indoor air exposome.

In this study, we analyzed previously collected samples and data from this natural experiment to better understand the range of VOCs and SVOCs that could be removed by CR boxes. To achieve a broader range of chemical coverage, we employed three NTA and SSA analytical methods: (1) liquid chromatography (LC) high resolution mass spectrometry (HRMS) with negative electrospray ionization (ESI), (2) LC-HRMS with positive ESI, and (3) gas chromatography (GC) HRMS with electron ionization. We categorized the tentatively identified candidates that decreased significantly into chemical classes or uses using EPA's CompTox Chemicals Dashboard [10] or by examining their proposed chemical structure. The results of our NTA and SSA provide a more complete characterization of unknown or suspected indoor air pollutants and the impact of a relatively low-cost intervention on their relative concentrations.

MATERIALS AND METHODS

Setting and study design

Details of the study design, including a description of the building in which the sampling took place, CR box construction, CR box operation, are provided in Dodson et al. [8]. We took advantage of a natural experiment that occurred between October 2021 – March 2022 to quantify changes in air concentrations of PFAS and other SVOCs before and during the deployment of CR Boxes. The study took place in the Brown University School of Public Health (Providence, Rhode Island, USA), an 11-story office building built in 1984. Each floor in the entire building receives outside air at a constant ventilation rate (approximately three to four air changes per hour) from side louvers that is sent to an air handling unit with MERV-13 filtration. The 17 classrooms, conference rooms, and computer labs where the study took place were spread across seven floors of the building and were all carpeted. In rooms with windows, the windows were inoperable. Characteristics of the room, including room area, presence and number of windows, type and number of furnishings, maximum number of occupants, and number of electronics in each room were previously reported [8].

We conducted baseline sampling between October 25, 2021 and November 18, 2021. One week after baseline sampling completion, we deployed the CR boxes and operated them from 0700 to 1900 on weekdays until December 20, 2021. We placed one to three CR Boxes in each room, near walls and in some cases corners to reduce interference with foot traffic, depending on the room area so that the fans provided approximately six additional effective air changes per hour. CR boxes were turned off during the winter break (December 21, 2021 through January 24, 2022), except in some conference rooms used by staff during the break. Intervention sampling began two weeks after the CR boxes were turned back on (February 7, 2022 through March 4, 2022). CR boxes were again operated from 0700 to 1900 on weekdays.

We collected air samples twice in each room, one baseline sample and one sample following the installation of CR boxes. Air samples were collected in the same manner before and during the intervention. In both instances, we sampled the air in a staggered fashion by collecting three to five samples per week in different rooms of the building. The building was occupied before and during intervention as classes were in session. Building occupants were aware of the study and its goals. During air sampling periods, we posted signs

requesting that custodial staff not clean in the rooms and occupants to refrain from using perfume, cosmetics, or aerosols in the rooms.

SVOC air sampling

Active air sampling was conducted in each room using previously described methods [11, 12]. In total, 34 field samples were collected, including 17 before the intervention and 17 during the intervention. Two field blanks were collected and three technical field replicates were collected. Briefly, we sampled gas and particulate phases using parallel 160mm Universal Research Glassware (URG) personal pesticide samplers (URG); Chapel Hill, NC) at a 3 L/min flow rate over ~96 h. Air flow rate was measured at the beginning and end of each sampling period using a Model 4199 air flowmeter (TSI Incorporated; Shoreview, MN). Each sampler contained a 10 μm at 4 L/min impactor-equipped inlet followed by a 25mm quartz fiber filter and 3g of XAD-2 resin sandwiched between two 1 13/16 in. polyurethane foam (PUF) plugs (Fisher Scientific, Waltham MA). Prior to packing, the PUF plugs and XAD-2 resin were washed with UHPLC grade acetonitrile (Sigma-Aldrich; St. Louis, MO) and dried in a 60 °C oven for 3 days. After sample collection, the samplers were capped, stored in sealed bags, and stored for less than 5 months at −20 °C.

We measured room air temperature and relative humidity using Purple Air Monitors (Draper, Utah) both before and during the intervention. We averaged hourly temperature and relative humidity values for each room in the before and during intervention periods for use in subsequent statistical analyses.

Sample preparation

Our analysis used the XAD-2 resin and PUF plugs in the air sampler, which captured pollutants in the gas-phase and not the particle-bound phase. Prior to extraction, XAD-2 resin and PUF plugs were removed from the air samplers and weighed in 50 mL glass centrifuge tubes. The extraction method was validated for PFAS, phthalates, OPEs, polychlorinated biphenyls, and polybrominated diphenyl ethers in our original targeted study [8]. The PUF and XAD-2 resin powder were extracted with three 10-mL (30mL total) washes of acetonitrile. The acetonitrile supernatant was collected in a separate 50 mL glass centrifuge tube. Two 1 mL aliquots of the supernatant were collected for analysis using GC-HRMS and LC-HRMS. The fraction used for LC-HRMS was transferred to a HDPE analysis vial, spiked with 300 μL aqueous isotopically labeled PFAS internal standard (IS) (40 μg/L; contents in the SI and Table S1), and reduced to 300 μL using a Organomation 30-position Multivap Nitrogen Evaporator (Organomation Associates Inc.). The GC-HRMS fraction was transferred to a glass vial, spiked with 10 μL of a solution containing isotopically labeled phthalates (40 μg/L Diethyl Phthalate-3,4,5,6-d4, Diisobutyl Phthalate-3,4,5,6-d4, Di-n-pentyl phthalate-3,4,5,6-d4, Di-n-hexyl Phthalate-3,4,5,6-d4, and Di-n-octyl Phthalate-3,4,5,6-d4 in acetonitrile), and reduced to 150 μL under nitrogen. The final extract was transferred to an amber autosampler vial containing a 250 μL glass insert and sealed with a cap. The extract that was used for GC analysis was spiked with 10 μl of an IS solution containing 62.5 μg/L of phenanthrene D-10, 62.5 μg/L chrysene D-12, and 20 μg/L retention time marker in hexane. The isotope labeled phenanthrene and chrysenes were used to monitor injection consistency, while the retention time marker was used for retention

time alignment and calculating Retention Index in NTA/SSA. All chemicals and materials used are listed in the SI.

QC spikes and samples

We collected and analyzed several blanks and replicates to evaluate potential contamination and precision of our SVOC sampling. We collected both solvent blanks and field blanks (samplers opened in a room and then processed, one before and one during CR Box deployment). Solvent blanks were used to determine the method detection limit (MDL). Three technical field replicates were collected by simultaneously sampling in a single residence using the same procedures. Recoveries of PFAS, phthalates, organophosphate esters, polychlorinated biphenyls, and polybrominated diphenyl ethers were assessed as a part of our targeted study (reported in the SI) [8] by spiking a known amount of analytical standard into the XAD and PUF used for sampling. The recoveries were between 70 and 110%. The intended use of the QC samples was to monitor instrument performance.

Analytical sequence

For all three HRMS platforms (LC with negative ESI, LC with positive ESI, and GC-HRMS), samples were analyzed in a randomized order with pre- and during intervention samples mixed together. Blank samples and a calibration standard were analyzed every 10 injections to evaluate changes in PFAS, phthalates, organophosphate esters, polychlorinated biphenyls, and polybrominated diphenyl ethers peak area. The calibration standard also contained 11 certified references standard mixtures (listed in the SI). The three technical replicate samples were analyzed at the beginning, middle, and end of the batch. All samples were analyzed in a single batch, so no batch correction was performed. We used Thermo TraceFinder 4.0 software to monitor performance (e.g., standard and IS peak area and retention time) throughout the analytical sequence.

Instrumental analysis

For the two LC schemes, data was collected on a high resolution Thermo QExactive HF-X Orbitrap MS equipped with a Vanquish ultra-high-performance liquid chromatograph. The primary goal of the original targeted study was to detect changes in semi-volatile PFAS and therefore we based the chromatography on EPA Draft Method 1633 [8, 13]. For both ionization modes, we used a Thermo Hypersil Gold Vanquish C18 column (100 mm × 2.1 mm × 1.9 μm) for chromatography, ESI, and data-dependent (dd) MS^2 acquisition. Fragmentation was performed in the HCD collision cell filled with N_2 (produced by a Peak Scientific Nitrogen Generator, Genius NM32LA). All instrument parameters, including the chromatography scheme, source settings, full scan parameters, and data dependent (dd) MS^2 settings, for both negative and positive ESI are provided in the SI (Table S2). The instrument was calibrated immediately before both the negative and positive ESI analytical sequence.

GC-HRMS analysis was performed using methods we previously developed [14] for a high-resolution Thermo Q Exactive Orbitrap MS equipped with a Thermo Trace 1300 GC and a TriPlus RSH Autosampler. Sample extracts (2 μL) were injected onto a 290 °C split/splitless inlet operated in split-less mode, components were separated on a Restek Rxi-35Sil MS column (30m × 0.25mm inner diameter × 0.25 μm film thickness) column, and data

was acquired in full-scan mode. The MS was operated in full scan with electron ionization mode (70 eV). Helium (99.9% purity) and nitrogen (99.9% purity) were the carrier and c-trap gases, respectively. Full details of the inlet settings, chromatography scheme, and MS settings are provided in the SI (Table S3). The instrument was leak checked, tuned, and calibrated immediately before the analytical sequence.

Data processing

All spectral data files were saved in the .RAW file format and NTA/SSA was performed in Thermo Compound Discoverer (CD) 3.3 software. To evaluate CD settings, we analyzed the calibration samples to evaluate workflow parameters (e.g., mass accuracy, retention time, peak area). The CD data processing workflow and nodes for all three HRMS platforms are provided in the SI (Figs. S1, S2, and S3). Briefly, for LC-HRMS data (positive and negative ionization), peaks were detected with 5 ppm mass tolerance, 10,000 minimum peak intensity, and signal to noise threshold of 1.5. For GC-HRMS data, peaks were detected with 10 ppm mass tolerance, 100,000 total ion chromatogram threshold, signal to noise ratio of 3, and 98% allowable ion overlap. Each chromatogram was retention time aligned using the carbon distribution marker (contains 9 alkanes; only compounds containing greater than 8 carbons were used since the compounds smaller than this eluted during the solvent delay) spiked into each sample and retention indices were calculated for each peak detected. The peak area for each putatively identified compound detected was exported to Microsoft Excel after processing the raw data and prior to data filtering.

In total, we processed 8 extraction blanks, 3 calibration standards, 3 QA/QC samples, and 34 air samples for each analytical platform. Peak areas detected in blank samples were excluded from the experimental samples if the sample peak area was less than the MDL. When the blank samples had no peak area in any replicates, the MDL was zero. When the blank samples had peak area in at least one sample, but not all 8, the MDL was set to the maximum peak area detected in the blank. When the blank samples had peak area in all blank samples, the MDL was calculated using $MDL = \overline{X} + t_{(n-1,1-\alpha=0.99)}S_b$, where $\overline{X}$ is the method blank peak areas mean, $t_{(n-1,1-\alpha=0.99)}$ is the student's t value for the single-tailed 99th percentile t-statistic with $n-1$ degrees freedom, and S_b is the sample standard deviation of replicate blanks peak area [15]. We then removed features that had coefficients of variation (CV) greater than 30% in the QA/QC replicates.

Compound annotation and harmonization of identification confidence levels

We assigned confidence levels to the putatively identified compounds based on the Schymanski Scale (LC) or the Actionable Annotation Scoring Framework for GC-HRMS by Koelmel et al. to evaluate the certainty of the structure identification [16, 17]. Given that these scales have different sub-levels (i.e., Schymanski has levels 2a and 2b, while Koelmel has levels 4a, 4b, and 4c) and the inherent differences in GC and LC data, we did not harmonize at the sub-level across methods. Additional details on how confidence levels and high resolution mass spectral libraries (e.g., in-house and open libraries [18]) were assigned is provided in the SI.

Statistical analysis and categorization

Statistical analysis was performed using R (version 4.0.3). Prior to statistical analysis, we removed features with ≥20% missingness (or non-detect) in either pre- or during-intervention samples from further analysis (i.e., no feature was detected or was <MDL in ≥4 samples). For features with <20% missingness, we replaced missing values with MDL/sqrt(2) [19]. Each area count was standardized by the volume of air that passed through the sampling device (units of area count per m^3). The air volume standardized area counts were $\log_2$-transformed to approximate normality assumptions in subsequent regression models.

We compared feature area counts before and during the intervention using two sets of analyses. First, we applied principal component analysis using the *prcomp* and *pca3d* R packages with default settings to each data set to reduce the dimensionality of the dataset and examine the effect of the intervention by examining biplots of the first two PCs [20].

Second, we used the following linear mixed effects models with a random intercept for the room to estimate the difference in feature area count before and during the intervention.

$$Y_{ijk} = \beta_0 + \beta_1 X_1 + b_{oi} + \beta_l X_{ijl}$$

In this model, Y_{ijk} is the log2-transformed area count for the k-th feature in the i-th room (i = 1 to 17) at the j-th time (j = 0, 1). β_0 is the model intercept and b_{oi} is the room specific deviation in the intercept. β_1 is the difference in log2-transformed area count for the respective feature with x_1 set to 0 for the pre-intervention period and 1 for the during-intervention period. $\beta_l X_l$ represent beta coefficients and time-varying temperature and relative humidity for the i-th room at the j-th time. We used β_1 to calculate percent difference (100 × (2^β_1 −1)) and the 95% confidence interval for percent difference (100 × (2^(β_1 ± 1.96 SE) −1)), where SE is the standard error.

Resulting p values from β_1 were adjusted for multiple comparisons using a 20% FDR. We created interactive volcano plots using the Plotly R package [21]. Features that resulted in adjusted p-values less than the 20% FDR and fold-change (FC) ≤−1 (i.e., ≥50% decrease) were considered to be significantly decreased during the intervention. Features considered to increase significantly had adjusted p values less than the 20% FDR and fold-change (FC) ≥ 1 (i.e., ≥100% increase).

Significantly decreased identified and putatively identified features were categorized using EPA CompTox Chemicals Dashboard [10], which we have previously described [14]. Briefly, the batch search routine was used to search the tentatively identified chemicals. All lists (337 lists at the time we downloaded them from CompTox Chemicals Dashboard) that were currently available were used to categorize the identified chemicals into groups. Lists that did not include a chemical purpose or a chemical class (e.g., targeted MS lists contributed by other labs) were then excluded. When the chemical was not found on the CompTox Chemicals Dashboard, we categorized the chemical using information from the Abstract Sifter tool [22] or structural information from PubChem [23] or ChemSpider [24]. When the chemical could not be classified, the purpose or class was classified as “unknown.”

RESULTS

Across all three analytical methods (LC-HRMS in positive and negative ionization and GC-HRMS), 9,387 features were detected across all 34 samples (Table 1). After removing features detected in less than 80% of the pre- or post-intervention samples and those that did not have CVs <30% in the QA/QC samples, 2471 features were included in further statistical analysis.

Using the Schymanski scale [16] for both LC-HRMS methods and the Actionable Annotation Scoring Framework for GC-HRMS by Koelmel et al. [25], we assigned confidence levels to the identified and putatively identified features in the unfiltered feature table (Table 1). Overall, 63.5% of the features across all three techniques were Confidence Level 3 (at least a tentative candidate) or higher. We obtained higher confidence levels for features putatively identified in LC-HRMS in negative ionization mode (85.5% Level 3 or higher) and LC-HRMS in positive ionization mode (80.8% Level 3 or higher) compared to GC-HRMS (37.9% Level 3 or higher). We identified 60 compounds with a Confidence Level of 1 (Table S4). Level 1 annotations were observed in LC-HRMS negative ionization and GC-HRMS. In LC-HRMS negative ionization, 19 compounds were annotated with Level 1 confidence. In GC-HRMS, 41 compounds were annotated with Level 1 confidence. Of these compounds, we targeted 33 in our original study [8]. After filtering for missingness and QA/QC suitability, 22 of the Level 1 annotated compounds were retained in the feature table used for statistical analysis (Table 1 and S5).

Using bi-plots of the first two principal components (PCs), we observed clustering of the rooms based on the intervention period. For LC-HRMS negative ionization, there was clear separation of observations that aligned with samples taken before vs. during intervention (Fig. 1a). The first two PCs cumulatively explained 24.7% of the variation in features detected. There was less clear separation for samples taken before vs. during the intervention for data collected in positive ionization mode for LC-HRMS (Fig. 1b). In LC-HRMS positive ionization mode, the first two PCs cumulatively explained 34.2% of the variation in features. For GC-HRMS, before intervention samples clustered tightly together and overlapped with the cluster of samples taken after the intervention (Fig. 1c). In GC-HRMS, the first two PCs cumulatively explained 25.4% of the variation in features. These findings indicate that features measured in LC-HRMS negative ionization mode, and to a lesser extent GC-HRMS, differed before and during the intervention.

From all three analytical methods, 89.4% of the total number of features in the filtered feature tables decreased by at least 50% regardless of statistical significance. In each analytical method, the proportion of features that declined by at least 50% were: 75.1% for LC-HRMS with negative ionization, 69.9% for LC-HRMS with positive ionization, and 95.3% for GC-HRMS (Table 1).

Across all three analytical platforms, 71 features decreased significantly (FDR p value < 0.2, >50% decrease): 11 from LC-HRMS negative ionization, 4 from LC-HRMS positive ionization, and 56 from GC-HRMS (Table 2, Fig. 2; an interactive version of this figure is also available in the SI). Of these, four features were Level 1 annotations

(diisobutyl phthalate, dimethyl phthalate, PFBS, and safrole), one feature was a Level 2 annotation (putative identifications: 2,5-di-tert-butylhydroquinone, dibenz[a,j]anthracene, and pentaphene), 33 were Level 3, nine were Level 4, and 22 were Level 5. One of the significant features was detected in both LC-HRMS negative and positive ionization with the same retention time (4.284 min) and had the same putative annotation, 5-(benzyloxy)-2-piperazinopyrimidine.

The percent decreases of these 71 features ranged from 50 to 100%, with a median percent decrease of 68.6%. In LC-HRMS negative ionization, one of the three chemicals with the greatest percent decrease was PFBS (Level 1) (−100%, 95% CI: −108, −91.4). The other two features were putatively identified as tris(2,4-ditert-butylphenyl)phosphate (Level 3) (−99%, 95% CI: −104, −95.6) and 2,5-di-tert-Butylhydroquinone (Level 2) (−99%, 95% CI: −107, −92.1). In LC-HRMS positive ionization, the most significantly decreased features during the intervention were putatively identified as 1-[4-(Diphenylmethyl)-1-piperazinyl]-3-[(2-phenylethyl)amino]-2-propanol (Level 4) (−100%, 95% CI: −107, −92.7), 4-(3-(4-Piperidyl)propyl)-1-piperidineethanol (Level 3) (−99%, 95% CI: −107, −92.5), and5-(benzyloxy)-2-piperazinopyrimidine (Level 3) (−99%, 95% CI: −107, −92.5). In GC-HRMS, the feature with the greatest percent decrease (−99%, 95% CI: −96.4, −103) was putatively identified as furathiocarb (Level 3).

After categorizing the 49 identified and putatively identified chemicals (22 features were Level 5 and could not be categorized) that declined during the intervention into their uses or chemical classes, we identified and putatively identified one disinfectant; nine fragrance and/or food chemicals; four nitrogen-containing heterocyclic compounds; one OPE; eight Polycyclic Aromatic Hydrocarbons (PAHs); one PCB; 18 pesticide, herbicide, or insecticide chemicals; two PFAS; three phthalates; and two plasticizers (Table 2, Fig. 3). From each category, the identified and putatively identified chemicals declined by 77.8–99%. Of the putatively identified nitrogen-containing heterocyclic compounds, three had 100% percent decrease (Table 2).

In LC-HRMS negative ionization, there was no chemical class that represented the majority of significantly decreased, identified and putatively identified chemicals. The two categories with the greatest number of chemicals in negative ionization were PFAS and phthalates (n = 2) (Fig. 3). In LC-HRMS positive ionization, the majority of the identified and putatively identified chemicals were nitrogen-containing heterocyclic compounds (n = 3; 75.0%) (Fig. 3). In GC-HRMS, the majority of the significantly decreased, identified and putatively identified chemicals were pesticides, herbicides, or insecticides (n = 18; 48.6%) (Fig. 3).

Across all three analytical methods used, 2 m/z features significantly increased (FC ≥ 1 and p value < 20% FDR threshold) (Table S6). Both features were detected using GC-HRMS and could not be identified (Level 5 annotation). The percent difference of these features were 309% (95% CI: 307, 310) and 1,022% (95% CI: 1020, 1023).

DISCUSSION

Using a natural experiment, we found that CR boxes significantly reduced the indoor air abundance of 49 identified and putatively identified chemicals detected using NTA and SSA. We found that 22 additional features significantly decreased but were not identifiable (Level 5 annotation). In some cases, CR boxes reduced identified and putatively identified chemicals indoor air area counts by up to 99%. While the study objective was to understand the potential chemicals reduced by CR boxes, some features increased during the intervention. However, we were unable to obtain an identification for these two features.

In GC-HRMS, six of the putatively identified pesticides that decreased were carbamate compounds, which are widely used in indoor environments to treat insects, such as ants or cockroaches [26]. Carbamates are known endocrine disruptors and neurotoxins [27–29], and impair enzymatic pathways involved in metabolism of carbohydrates, fats, and proteins within cytoplasm, mitochondria, and peroxisomes by inhibiting acetyl cholinesterase enzymes [30]. Carbamates, including pirimicarb and isoprocarb, have been identified in indoor dust, dryer lint, and indoor plants [31, 32]. Thus, detection of these putatively identified compounds is consistent with prior studies detecting these compounds indoors. We obtained a list of the pesticides used in the building and none contained carbamides; however, many of the products only disclose a small portion (i.e., 10%) of their ingredients. Another entity managed the building up until June 2021, which may have used different products that persisted in the building and contributed to the indoor air quality. Bifenthrin, another significantly reduced putatively identified chemical, was a listed ingredient in two of the products currently used by the University for pest control. Thus, the CR boxes may be capable of reducing several pesticides in indoor air.

LC-HRMS (both negative and positive ionization) revealed reductions in putatively identified nitrogen-containing heterocyclic compounds; while GC-HRMS revealed reductions in putatively identified PAHs. Both PAHs and nitrogen-containing heterocyclic compounds are present in outdoor air, including urban environments, and are associated with atmospheric aerosols [33–36]. Nitrogen-containing heterocyclic compounds are produced as a result of vehicle emissions from biofuels and petroleum based fuels [37, 38] and are used in pesticides, roasted meats, chemical manufacturing, and pharmaceuticals [39–41]. Indoors, nitrogen-containing heterocyclic compounds have been detected in residential environment before and after cooking and in homes where bituminous coal combustion is used for cooking and/or heating [42, 43]. Additionally, nitrogen containing heterocyclic compounds were detected in homes with gas and electric furnaces and cooking appliances [44]. Similarly, PAHs are produced both indoors and outdoors as a product of any combustion involving fossil fuels, including transportation and cooking [45, 46]. There is one restaurant on the ground level of the office building where we collected these samples, so it is possible that the source of the putatively identified PAHs and nitrogen-containing heterocyclic compounds was related to indoor cooking. Another possible source of these putatively identified compounds is vehicle emissions. The building is located along two busy city streets and there is a multi-story parking ramp adjacent to the building. Additionally, there is a gas-fired power station less than 1 mile from the building where sampling took place. We found little to no information on the uses of the putatively identified nitrogen-

containing heterocyclic compounds that decreased significantly in this study; however, many of the putatively identified nitrogen-containing heterocyclic compounds contained piperazine or pyrimide functional groups, which are in pesticides, vehicle emissions, and cooking emissions [37, 42, 47].

We also putatively identified tris(2,4-ditert-butylphenyl)phosphate, an OPE, as a significantly decreasing chemical. Tris(2,4-ditert-butylphenyl)phosphate was previously detected in air samples [48]. OPEs are synthetic chemicals used as flame retardants and plasticizers, and they have been detected in the indoor environment [49]. While tris(2,4-ditert-butylphenyl)phosphate is an understudied OPE and its specific health effects are unknown, exposure to other OPEs is associated with endocrine disruption, neurotoxicity, and carcinogenicity [50]. In our original study, where three OPEs were targeted, these did not significantly decrease during the intervention, but we did detect increased OPE levels on the CR box filters after the intervention [8].

A few features increased during the intervention period, though we could not identify them. The reasons for the observed increases are unknown but could be due to behaviors of occupants in the building. Because we operated the CR boxes for 12 h each day but sampled the air continuously, some chemical concentrations may have increased when the filters were not operating.

While the health effects of some of the compounds detected in this study are unknown, the health effects of some pesticides and PAHs are established. Exposure to pesticides and PAHs are associated with a number of inhalation risks, including shortterm and chronic health effects [51, 52]. Some health effects of pesticide exposure include diabetes, cancer, skin and eye irritation, and nausea [51]. Health effects of PAH exposure include lung cancer, cardiovascular disease, hypertension, and oxidative stress, among other [52]. Prior studies have investigated the relationship of indoor air contaminant concentrations to concentrations in paired biological samples. Whyatt et al. examined the relationship between 29 pesticides in indoor air using personal air samplers and pesticide concentrations in plasma from 230 mother and newborn pairs. Air concentrations of some pesticides, including a carbamate (propoxur), were significantly correlated with plasma concentrations [53]. Similarly, a number of studies have found correlations between concentrations of PAHs in air (sampled using personal devices) and PAH biomarker levels in biological samples, including blood and urine [54]. Thus, CR boxes may reduce biomarker concentrations of these compounds and this could be investigated in future studies.

This study has several strengths. First, we performed a multi-method assessment of indoor air contaminants and harmonized LC-HRMS and GC-HRMS identification confidence scoring schemes. This allowed us to increase chemical coverage and detect compounds that we did not expect to detect a priori. We anticipated that LC-HRMS would not reveal detectable changes, since this technique is more amenable to less volatile compounds than GC-HRMS. However, the inclusion of LC-HRMS allowed us to identify a significant decrease in the novel OPE tris(2,4-ditert-butylphenyl)phosphate that has previously been associated with $PM_{2.5}$ [48] and several nitrogen-containing heterocyclic compounds. Second, we conducted this study over a relatively short period of time in a single building

to reduce time-varying confounding. Third, we took advantage of a natural experiment to estimate potential causal effects of the CR boxes on indoor air pollution. An alternative approach could have sampled rooms that did not receive the intervention to ensure unmeasured time-varying factors did not influence the results.

Our study also has some limitations. This natural experiment was not performed in a controlled environment and time-varying factors that we did not adjust for, such as occupancy or occupant behavior, may have affected indoor air pollutant abundance. Thus, time-varying factors that covaried with the intervention could be responsible for the observed reductions in feature abundance. Additionally, operation of the CR boxes increased the noise level in the rooms and occupants occasionally turned off the CR box during the intervention because of noise concerns. This may result in an underestimation of the true reductions in indoor air contaminant levels. While spurious findings arising from multiple comparisons are a concern, we corrected p values to control for false discovery and present all our findings to avoid selective reporting. Moreover, our pattern of results show that many compounds decreased during the intervention period, albeit not at FDR < 0.2, particularly for those detect with GC-HRMS. Finally, while we used a multi-method approach to increase chemical coverage of VOCs and SVOCs, our methods were initially optimized for our targeted study, which included PFAS, phthalates, BDEs, PCBs, and some OPEs. This could bias our analysis toward compounds with similar physical-chemical properties. Furthermore, we did not perform post-hoc validation of the putatively identified chemicals that significantly decreased due to the cost and time related to obtaining certified reference standards.

In conclusion, CR boxes significantly decreased relative abundance of 49 identified or putatively identified indoor air chemicals, including pesticides, herbicides, or insecticides, PAHs, PFAS, and nitrogen-containing heterocyclic compounds. The decreases in several of these compounds, including a novel OPE, disinfectant, and pesticide exemplifies the importance of including NTA and SSA in exposure assessment studies to more comprehensively assess the impact of interventions on the indoor air exposome. Classifying the features that decreased during the intervention provided additional information on the types of chemicals removed by CR box operation and demonstrated that each analytical method covered a different chemical space. This study provides the basis for future studies designed to test interventions to improve indoor air quality and human health, as many of the chemicals we putatively identified in this study are related to adverse health outcomes. While humans may be exposed to these pollutants through other sources (e.g., drinking water, consumer products, food), CR boxes offer a relatively inexpensive means to reduce personal chemical exposure to indoor air contaminants.

Supplementary Material

Refer to Web version on PubMed Central for supplementary material.

ACKNOWLEDGEMENTS

We would like to thank Emilia G. Braun and Elissia Franklin for their assistance with the field work; Kevin Travossos for providing us with detailed information about the building's air handling system; Jim Rosenthal

providing us with information about the composition of the Tex-Air filters; and Youn Kyeong Chang and Roberta De Vito for discussing statistical approaches for analyzing the data. We are grateful for funding from the Brown School of Public Health Dean's Office and Health Equity Scholars Program. This manuscript was evaluated against the NTA Study Reporting Tool (SRT) during peer-review (Peter et al., 2021; DOI: 10.1021/acs.analchem.1c02621).

FUNDING

Funding for this work came from the Brown University School of Public Health. JMB and KM were supported by NIEHS R01 ES032386. The Thermo LC-Orbitrap MS was partially funded by NSF Major Research Instrumentation (MRI) award CBET-1919870 to KDP.

DATA AVAILABILITY

The data generated during this study can be found within the published article and its supplementary files. Supplementary information is available at the Journal of Exposure Science & Environmental Epidemiology's website.

REFERENCES

1. Spengler JD, Sexton K. Indoor air pollution: a public health perspective. Science. 1983;221:9–17. [PubMed: 6857273]
2. Wild CP. Complementing the genome with an "exposome": the outstanding challenge of environmental exposure measurement in molecular epidemiology. Cancer Epidemiol, Biomark Prev. 2005;14:1847–50.
3. Hoskins JA. Health effects due to indoor air pollution. Indoor Built Environ. 2003;12:427–33.
4. Bernstein JA, Alexis N, Bacchus H, Bernstein IL, Fritz P, Horner E, et al. The health effects of nonindustrial indoor air pollution. J Allergy Clin Immunol. 2008;121:585–91. [PubMed: 18155285]
5. Wallace LA, Pellizzari ED, Hartwell TD, Sparacino C, Whitmore R, Sheldon L, et al. The TEAM study: personal exposures to toxic substances in air, drinking water, and breath of 400 residents of New Jersey, North Carolina, and North Dakota. Environ Res. 1987;43:290–307. [PubMed: 3608934]
6. Ma J, McHugh T, Beckley L, Lahvis M, DeVaull G, Jiang L. Vapor intrusion investigations and decision-making: a critical review. Environ Sci Technol. 2020;54:7050–69. [PubMed: 32384239]
7. González-Martín J, Kraakman NJR, Pérez C, Lebrero R, Muñoz R. A state–of–the-art review on indoor air pollution and strategies for indoor air pollution control. Chemosphere. 2021;262:128376. [PubMed: 33182138]
8. Dodson RE, Manz KE, Burks SR, Gairola R, Lee NF, Liu Y, et al. Does using corsi–rosenthal boxes to mitigate COVID-19 transmission also reduce indoor air concentrations of PFAS and phthalates? Environ Sci Technol. 2023;57:415–27. [PubMed: 36562547]
9. Dal Porto R, Kunz MN, Pistochini T, Corsi RL, Cappa CD. Characterizing the performance of a do-it-yourself (DIY) box fan air filter. Aerosol Sci Technol. 2022;56:564–72.
10. Williams AJ, Grulke CM, Edwards J, McEachran AD, Mansouri K, Baker NC, et al. The CompTox Chemistry Dashboard: a community data resource for environmental chemistry. J Cheminform. 2017;9:61. [PubMed: 29185060]
11. Dodson RE, Camann DE, Morello-Frosch R, Brody JG, Rudel RA. Semivolatile organic compounds in homes: strategies for efficient and systematic exposure measurement based on empirical and theoretical factors. Environ Sci Technol. 2015;49:113–22. [PubMed: 25488487]
12. Dodson RE, Udesky JO, Colton MD, McCauley M, Camann DE, Yau AY, et al. Chemical exposures in recently renovated low-income housing: Influence of building materials and occupant activities. Environ Int. 2017;109:114–27. [PubMed: 28916131]
13. Draft Method 1633 Analysis of per- and polyfluoroalkyl substances (PFAS) in aqueous, solid, biosolids, and tissue samples by LC-MS/MS. In: United States Environmental Protection Agency 2021.

14. Manz KE, Yamada K, Scheidl L, La Merrill MA, Lind L, Pennell KD. Targeted and nontargeted detection and characterization of trace organic chemicals in human serum and plasma using QuEChERS extraction. Toxicol Sci. 2022;185:77–88.
15. EPA U Definition and procedure for the determination of the method detection limit, Revision 2. Environmental Protection Agency EPA 2016.
16. Schymanski EL, Jeon J, Gulde R, Fenner K, Ruff M, Singer HP, et al. Identifying small molecules via high resolution mass spectrometry: communicating confidence. Environ Sci Technol. 2014;48:2097–8. [PubMed: 24476540]
17. Koelmel JP, Xie H, Price EJ, Lin EZ, Manz KE, Stelben P et al. An actionable annotation scoring framework for gas chromatography–high-resolution mass spectrometry (GC-HRMS). Exposome 2022; 10.1093/exposome/osac007.osac007.
18. Price EJ, Palát J, Coufaliková K, Kukučka P, Codling G, Vitale CM, et al. Open, high-resolution EI+ spectral library of anthropogenic compounds. Front Public Health. 2021;9:622558. [PubMed: 33768085]
19. Hornung RW, Reed LD. Estimation of average concentration in the presence of nondetectable values. Appl Occup Environ Hyg. 1990;5:46–51.
20. Weiner J, Weiner MJ Package 'pca3d'. 2017.
21. Sievert C Interactive web-based data visualization with R, Plotly, and Shiny. (CRC Press: London, England, 2020).
22. Baker N, Knudsen T, Williams A. Abstract Sifter: a comprehensive front-end system to PubMed. F1000Research. 2017;6:2614.
23. Kim S, Chen J, Cheng T, Gindulyte A, He J, He S, et al. PubChem in 2021: new data content and improved web interfaces. Nucleic Acids Res. 2021;49:D1388–D1395. [PubMed: 33151290]
24. Pence HE, Williams A. ChemSpider: an online chemical information resource. J Chem Educ. 2010;87:1123–4.
25. Koelmel JP, Xie H, Price EJ, Lin EZ, Manz KE, Stelben P, et al. An actionable annotation scoring framework for gas chromatography-high-resolution mass spectrometry. Exposome. 2022;2:osac007. [PubMed: 36483216]
26. Grossman J What's hiding under the sink: dangers of household pesticides. Environ Health Perspect. 1995;103:550–4. [PubMed: 7556005]
27. Moreira S, Silva R, Carrageta DF, Alves MG, Seco-Rovira V, Oliveira PF, et al. Carbamate pesticides: shedding light on their impact on the male reproductive system. Available from: URL (Accessed n Date Accessed Year)|.
28. Gea M, Zhang C, Tota R, Gilardi G, Di Nardo G, Schilirò T. Assessment of five pesticides as endocrine-disrupting chemicals: effects on estrogen receptors and aromatase. Int J Environ Res Public Health. 2022;19:1959. [PubMed: 35206146]
29. Mroz EA. Possible role of carbamates in neurotoxicity and neurotransmitter inactivation. Science. 1989;243:1615–1615. [PubMed: 2564700]
30. Karami-Mohajeri S, Abdollahi M. Toxic influence of organophosphate, carbamate, and organochlorine pesticides on cellular metabolism of lipids, proteins, and carbohydrates: a systematic review. Hum Exp Toxicol. 2011;30:1119–40. [PubMed: 21071550]
31. Liu S, Huang Y, Liu J, Chen C, Ouyang G. In vivo contaminant monitoring and metabolomic profiling in plants exposed to carbamates via a novel micro-extraction fiber. Environ Sci Technol. 2021;55:12449–58. [PubMed: 34494434]
32. Ouyang X, Weiss JM, de Boer J, Lamoree MH, Leonards PEG. Non-target analysis of household dust and laundry dryer lint using comprehensive two-dimensional liquid chromatography coupled with time-of-flight mass spectrometry. Chemosphere. 2017;166:431–7. [PubMed: 27705830]
33. Chibwe L, Manzano CA, Muir D, Atkinson B, Kirk JL, Marvin CH, et al. Deposition and source identification of nitrogen heterocyclic polycyclic aromatic compounds in snow, sediment, and air samples from the athabasca oil sands region. Environ Sci Technol. 2019;53:2981–9. [PubMed: 30741540]
34. Wang Z, Zhang J, Zhang L, Liang Y, Shi Q. Characterization of nitroaromatic compounds in atmospheric particulate matter from Beijing. Atmos Environ. 2021;246:118046.

35. Delhomme O, Millet M. Azaarenes in atmospheric particulate matter samples of three different urban sites in east of France. Atmos Environ. 2012;47:541–5.
36. Naumova YY, Eisenreich SJ, Turpin BJ, Weisel CP, Morandi MT, Colome SD, et al. Polycyclic aromatic hydrocarbons in the indoor and outdoor air of three cities in the U.S. Environ Sci Technol. 2002;36:2552–9. [PubMed: 12099449]
37. Obeid F, Van TC, Horchler EJ, Guo Y, Verma P, Miljevic B, et al. Engine performance and emissions of high nitrogen-containing fuels. Fuel. 2020;264:116805.
38. Later DW, Lee ML, Bartle KD, Kong RC, Vassilaros DL. Chemical class separation and characterization of organic compounds in synthetic fuels. Anal Chem. 1981;53:1612–20.
39. Padoley KV, Mudliar SN, Pandey RA. Heterocyclic nitrogenous pollutants in the environment and their treatment options—an overview. Bioresour Technol. 2008;99:4029–43. [PubMed: 17418565]
40. Sohail A, Al-Dalali S, Wang J, Xie J, Shakoor A, Asimi S, et al. Aroma compounds identified in cooked meat: a review. Food Res Int. 2022;157:111385. [PubMed: 35761641]
41. Hartman GJ, Jin QZ, Collins GJ, Lee KN, Ho CT, Chang SS. Nitrogen-containing heterocyclic compounds identified in the volatile flavor constituents of roasted beef. J Agric Food Chem. 1983;31:1030–3.
42. Zeng J, Yu Z, Mekic M, Liu J, Li S, Loisel G, et al. Evolution of indoor cooking emissions captured by using secondary electrospray ionization high-resolution mass spectrometry. Environ Sci Technol Lett. 2020;7:76–81.
43. Zhang J, Smith KR. Household air pollution from coal and biomass fuels in China: measurements, health impacts, and interventions. Environ Health Perspect. 2007;115:848–55. [PubMed: 17589590]
44. Chuang JC, Mack GA, Kuhlman MR, Wilson NK. Polycyclic aromatic hydrocarbons and their derivatives in indoor and outdoor air in an eight-home study. Atmos Environ Part B Urban Atmos. 1991;25:369–80.
45. Howsam M, Jones KC. Sources of PAHs in the environment. In: Neilson AH (eds) PAHs and related compounds. The handbook of environmental chemistry, vol 3/3I. (Springer, Berlin, Heidelberg, 1998).
46. Patel AB, Shaikh S, Jain KR, Desai C, Madamwar D. Polycyclic aromatic hydrocarbons: sources, toxicity, and remediation approaches. Front Microbiol. 2020;11:562813. [PubMed: 33224110]
47. Pereira PCG, Parente CET, Carvalho GO, Torres JPM, Meire RO, Dorneles PR, et al. A review on pesticides in flower production: a push to reduce human exposure and environmental contamination. Environ Pollut. 2021;289:117817. [PubMed: 34333268]
48. Shi J, Xu C, Xiang L, Chen J, Cai Z. Tris(2,4-di-tert-butylphenyl)phosphate: an unexpected abundant toxic pollutant found in PM2.5. Environ Sci Technol. 2020;54:10570–6. [PubMed: 32786564]
49. Okeme JO, Yang C, Abdollahi A, Dhal S, Harris SA, Jantunen LM, et al. Passive air sampling of flame retardants and plasticizers in Canadian homes using PDMS, XAD-coated PDMS and PUF samplers. Environ Pollut. 2018;239:109–17. [PubMed: 29649757]
50. Li J, Zhao L, Letcher RJ, Zhang Y, Jian K, Zhang J, et al. A review on organophosphate ester (OPE) flame retardants and plasticizers in foodstuffs: Levels, distribution, human dietary exposure, and future directions. Environ Int. 2019;127:35–51. [PubMed: 30901640]
51. Kim K-H, Kabir E, Jahan SA. Exposure to pesticides and the associated human health effects. Sci Total Environ. 2017;575:525–35. [PubMed: 27614863]
52. Mallah MA, Changxing L, Mallah MA, Noreen S, Liu Y, Saeed M, et al. Polycyclic aromatic hydrocarbon and its effects on human health: an overeview. Chemosphere. 2022;296:133948. [PubMed: 35151703]
53. Whyatt RM, Barr DB, Camann DE, Kinney PL, Barr JR, Andrews HF, et al. Contemporary-use pesticides in personal air samples during pregnancy and blood samples at delivery among urban minority mothers and newborns. Environ Health Perspect. 2003;111:749–56. [PubMed: 12727605]
54. Louro H, Gomes BC, Saber AT, Iamiceli AL, Göen T, Jones K, et al. The use of human biomonitoring to assess occupational exposure to PAHs in Europe: a comprehensive review. Available from: URL (Accessed n Date Accessed Year)|.

IMPACT STATEMENT:

- We used SSA and NTA to demonstrate that do-it-yourself Corsi-Rosenthal boxes are an effective means for improving indoor air quality by reducing a wide range of volatile and semi-volatile organic contaminants.

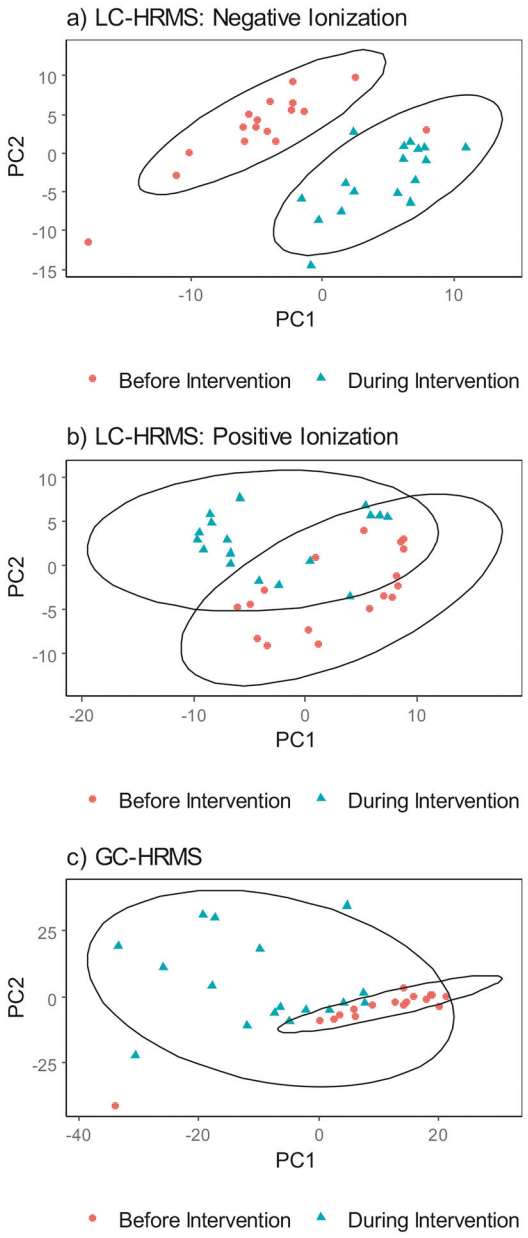

Fig. 1. Biplot of the first two principal components derived from features measured in air samples taken before and during the intervention.

PCA conducted separately on features from (**a**) LC-HRMS negative ionization, (**b**) LC-HRMS positive ionization, and (**c**) GC-HRMS. Each dot represents a single room before or during the CR box intervention. The shape and coloring represent whether the sample was taken before or during intervention. Ovals represent clustering among pre- and during intervention samples. In LC-HRMS negative ionization, 15.8% and 8.9% of the variance were explained by PCs 1 and 2, respectively. In LC-HRMS positive ionization, PCs 1 and 2 respectively explained 22.6% and 11.6% of the variance. In GC-HRMS, PCs 1 and 2 explained 14.1% and 11.3% of the variance, respectively.

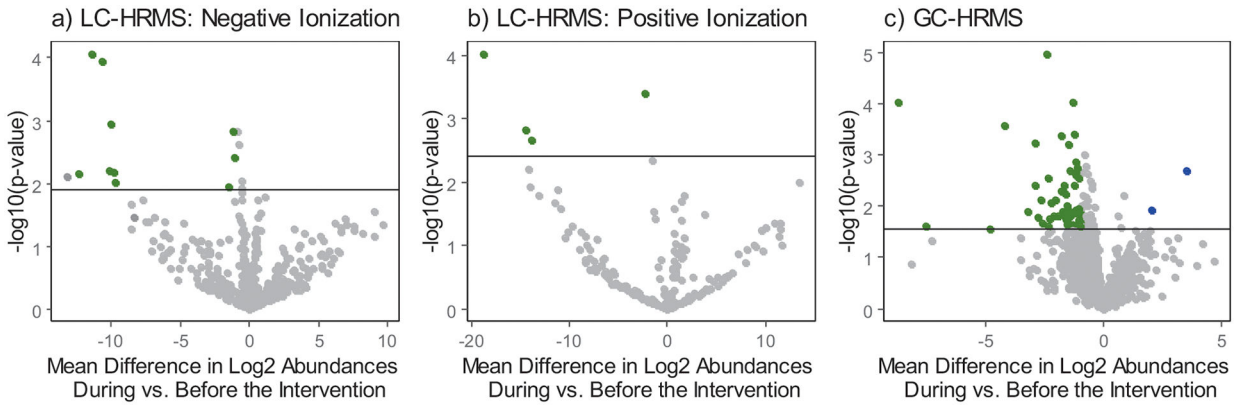

Fig. 2. Changes in feature intensity during the intervention.

Volcano plots for the features produced in (**a**) LC−HRMS negative ionization, (**b**) LC-HRMS positive ionization, and (**c**) GC-HRMS. Each dot represents a single feature. The solid black line is the 20% False Discovery Rate (FDR) threshold. The cut-off for the mean difference in log2 abundances during vs. before the intervention was ±1 features that at least doubled or halved in relative abundance). Points above this line with negative mean difference in log2 abundances (green dots, on the left side of the plots) are features that decreased significantly during the intervention (>50% decrease). Points above the FDR threshold with positive mean difference in log2 abundances (blue dots, on the right side of the plots) are features that increased significantly during intervention (>50% increase). Additional information about the individual features in these plots are available in interactive plots contained in the Supporting Information.

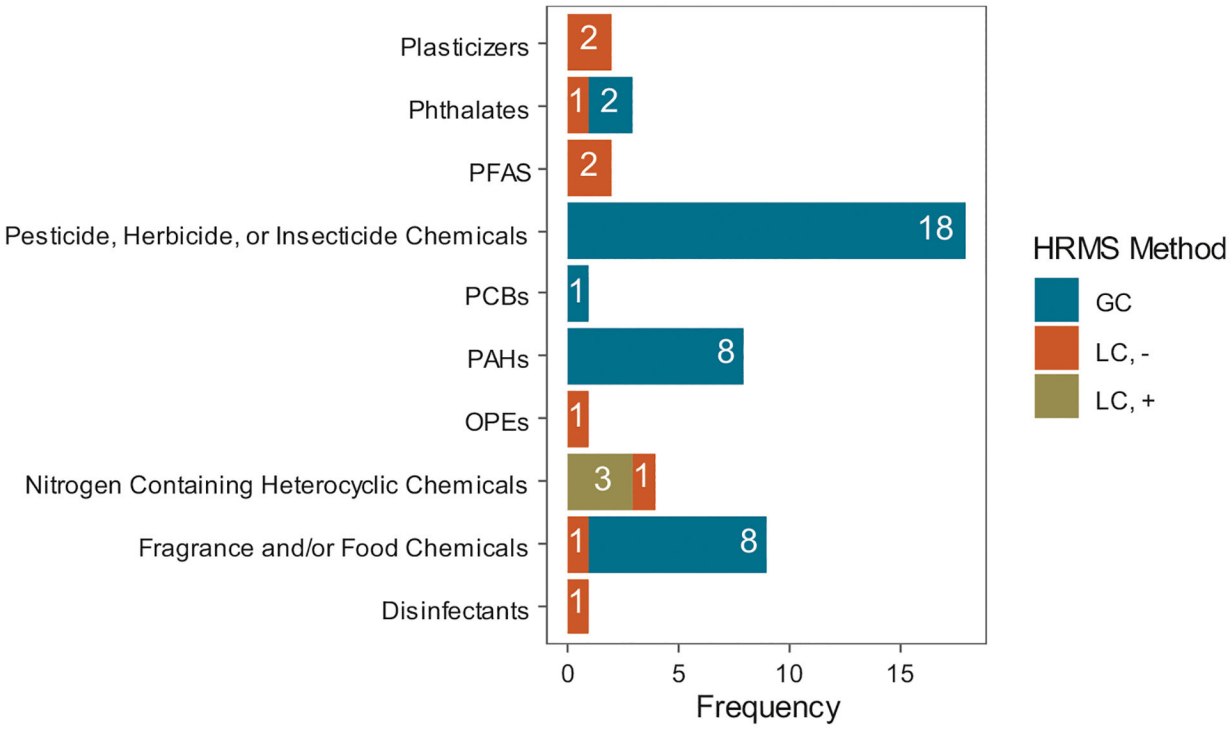

Fig. 3. Frequency of the types of compounds that significantly decreased (FDR *p* value < 0.2, >50% decrease) during CR intervention.

From the 71 features that significantly decreased, 49 were identified and putatively identified (Confidence Level >5, listed in Table 2, green points in Fig. 2 which have at least 50% decrease and a p-value less than the 20% False Discovery Rate (FDR) threshold) and were classified as: Disinfectants; Fragrance and/or Food Chemicals; Nitrogen-containing heterocyclic Chemicals; Organophosphate Esters (OPEs); Polycyclic aromatic hydrocarbons (PAHs); Polychlorinated Biphenyls (PCBs); Pesticide, Herbicide, or Insecticide Chemicals; Per- and Polyfluoroalkyl Substances (PFAS); Phthalates; or Plasticizers. The 22 features that significantly decreased and were Level 5 could not be categorized; thus are not included in this figure. The label on the bar chart indicates how frequently a chemical was categorized into the category on the y-axis for the specified analytical method.

Table 1.

Total number of features detected in each analytical platform or ionization mode and the confidence score in their identity.

		LC-HRMS		GC-HRMS
		Negative Ionization	**Positive Ionization**	**Electron Ionization**
Total number of features detected*:		3479	1731	4177
Total number of features included after filtering for				
1) >20% non-detect before or during intervention:		879	480	3,668
2) QC samples peak area CV <30%:		474	191	1806
Confidence levels[a] in the initial feature table:	1	19 (0.55%)	0 (0%)	41 (0.98%)
	2	197 (5.66%)	36 (2.08%)	13 (0.31%)
	3	2760 (79.3%)	1363 (78.7%)	1532 (36.7%)
	4	384 (11.0%)	241 (13.9%)	714 (17.1%)
	5	119 (3.42%)	91 (5.26%)	1877 (44.9%)
Confidence levels[a] in the filtered feature table:	1	3 (0.63%)	0 (0%)	19 (1.05%)
	2	64 (13.5%)	3 (1.57%)	4 (0.22%)
	3	341 (71.9%)	160 (83.8%)	714 (39.5%)
	4	57 (12.0%)	25(13.1%)	312 (17.3%)
	5	9 (1.90%)	3 (1.57%)	757 (41.9%)
Proportion of features that decreased[b]		75.1% (356)	69.6% (133)	95.3% (1721)
Proportion of features that increased[b]		24.9% (118)	30.4% (58)	4.71% (85)

*We used three analytical methods for NTA/SSA, LC-HRMS in negative ionization, LC-HRMS in positive ionization, and GC-HRMS in electron ionization.

[a]We harmonized to confidence scoring schemes, the Schymanski scale for LC-HRMS and the Actionable GC Scoring framework by Koelmel et al. Level 1 indicates a confirmed identification, Level 2 indicates a probable structure, Level 3 indicates a tentative candidate, Level 4 indicates a molecular formula or chemical group (for GC), and Level 5 indicates an unknown feature. The percentages represent the distribution of confidence scores in the filtered feature table.

[b]Proportion of features that decreased was calculated by determining the number of features with beta coefficients less than 1 (features with >50% decrease) divided by the total number of features in the final filtered feature table. Proportion of features that increased was calculated by determining the number of features with beta coefficients greater than 1 (features with >50% increase) divided by the total number of features in the final filtered feature table.

Table 2.

The 71 identified or putatively identified features that significantly decreased (FDR p value < 0.2, >50% decrease) during the CR Box intervention: Classified into categories based on their uses or chemical structure[a].

Identification or Putative Identification[a]	Formula	Analytical Method	Level	*p* value	Fold Change	% difference (95% Cl)
Disinfectants						
7-Chloro-1-phenazinecarboxylic acid	C13 H7 Cl N2 O2	LC, −	3	6.21×10^{-3}	−10.14	−99.9 (−106, −93.5)
Fragrance and/or Food Chemicals						
2,5-di-tert-Butylhydroquinone	C14 H22 O2	LC, −	2	6.89×10^{-3}	−12.38	−100 (−107, −92.1)
2-tert–Butyl-4-methoxyphenol	C11 H16 O2	GC	3	6.44×10^{-4}	−1.51	−65 (−65.7, −64.3)
Camphor	CIO H16 O	GC	3	5.17×10^{-3}	−1.77	−70.7 (−71.8, −69.6)
Cinnamyl alcohol	C9 H10 O	GC	4	9.35×10^{-5}	−1.31	−59.6 (−60.1, −59.1)
Coumarin	C9 H6 O2	GC	3	2.16×10^{-3}	−1.16	−55.3 (−55.9, −54.7)
Isomethyl-alpha-ionone	C14 H22 O	GC	3	2.00×10^{-3}	−1.43	−63 (−63.7, −62.2)
Lilail	C14 H20 O	GC	3	1.52×10^{-2}	−1.40	−62.1 (−63.1, −61.1)
Propyl decanoate	C13 H26 O2	GC	3	1.07×10^{-5}	−2.41	−81.2 (−82, −80.5)
Safrole	CIO H10 O2	GC	1	1.93×10^{-2}	−1.05	−51.8 (−52.6, −51)
Nitrogen Containing Heterocyclic Chemicals						
1-[4-(Diphenylmethyl)-1-piperazinyl]-3-[(2-phenylethyl)amino]-2-propanol	C28 H35 N3 O	LC, +	3	9.28×10^{-5}	−18.82	−100 (−107, −92.7)
4-(3-(4-Piperidyl)propyl)-1-piperidineethanol	C15 H30 N2 O	LC, +	3	1.49×10^{-3}	−14.49	−100 (−107, −92.5)
5-(benzyloxy)-2-piperazinopyrimidine	C15 H18 N4 O	LC, +	3	2.17×10^{-3}	−13.85	−100 (−107, −92.5)
5-(benzyloxy)-2-piperazinopyrimidine	C15 H18 N4 O	LC, −	3	1.16×10^{-3}	−10.04	−99.9 (−105, −94.9)
Organophosphate Esters (OPEs)						
Tris(2,4-ditert-butylphenyl)phosphate	C42 H63 O4 P	LC, −	3	8.61×10^{-5}	−11.45	−100 (−104, −95.6)
PAHs						
1,3-Dimethylnaphthalene	Cl2 HI2	GC	4	2.44×10^{-3}	−1.16	−55.4 (−56, −54.7)
1-Methylnaphthalene	C11 H10	GC	3	5.52×10^{-3}	−1.66	−68.3 (−69.4, −67.3)
1-Methylphenanthrene	C15 H12	GC	4	1.38×10^{-2}	−1.23	−57.3 (−58.2, −56.4)
2,3-Benzofluorene	Cl 7 H12	GC	3	1.24×10^{-2}	−1.49	−64.5 (−65.5, −63.4)

Identification or Putative Identification[a]	Formula	Analytical Method	Level	*p* value	Fold Change	% difference (95% CI)
Dibenz[a,j]anthracene	C22 H14	GC	2	5.96×10^{-3}	−1.59	−66.8 (−67.7, −65.8)
Pentaphene	C22 H14	GC	2	1.61×10^{-2}	−1.69	−69.1 (−70.3, −67.8)
Retene	C18 H18	GC	3	2.79×10^{-3}	−1.07	−52.3 (−52.9, −51.7)
Triphenylene	C18 H12	GC	3	7.61×10^{-3}	−2.01	−75.2 (−76.5, −73.9)
PCBs						
2,3-Dichlorobiphenyl	Cl 2 H8 CI2	GC	4	1.27×10^{-2}	−3.23	−89.4 (−91.6, −87.1)
Pesticide, Herbicide, or Insecticide Chemicals						
Aminocarb	C11 H16 N2 O2	GC	3	2.69×10^{-4}	−4.22	−94.6 (−96.4, −92.8)
Bifenthrin	C23 H22 Cl F3 O2	GC	3	7.77×10^{-3}	−2.68	−84.4 (−86.2, −82.7)
cis-Prallethrin	Cl9 H24 O3	GC	3	1.46×10^{-2}	−1.41	−62.3 (−63.3, −61.2)
Cycluron	C11 H22 N2 O	GC	3	9.95×10^{-3}	−1.53	−65.4 (−66.4, −64.4)
Cyphenothrin	C24 H25 N O3	GC	4	2.76×10^{-2}	−1.50	−64.7 (−65.9, −63.5)
Dioxacarb	C11 H13 N O4	GC	4	1.71×10^{-2}	−2.75	−85.1 (−87.2, −83.1)
Fenazaquin	C20 H22 N2 O	GC	3	4.01×10^{-3}	−1.68	−68.9 (−69.8, −67.9)
Fenobucarb	Cl 2 H17 N O2	GC	3	2.84×10^{-3}	−2.33	−80.2 (−81.5, −78.9)
Furathiocarb	C18 H26 N2 O5 S	GC	3	9.32×10^{-5}	−8.65	−99.8 (−103, −96.4)
Isoprocarb	C11 H15 N O2	GC	3	1.80×10^{-2}	−2.27	−79.3 (−81, −77.6)
lambda-Cyhalothrin	C23 H19 Cl F3 N O3	GC	4	1.75×10^{-2}	−1.60	−67 (−68.2, −65.8)
Mepronil	Cl 7 H19 N O2	GC	3	1.24×10^{-2}	−1.20	−56.5 (−57.3, −55.7)
Pirimicarb	C11 H18 N4 O2	GC	3	3.90×10^{-3}	−2.92	−86.8 (−88.5, −85)
Promecarb	Cl 2 H17 N O2	GC	4	2.80×10^{-2}	−4.78	−96.4 (−100.3, −92.5)
Pyracarbolid	C13 H15 N O2	GC	3	1.30×10^{-2}	−1.01	−50.4 (−51.1, −49.7)
Pyraclostrobin	C19 H18 Cl N3 O4	GC	3	2.08×10^{-2}	−1.53	−65.4 (−66.5, −64.2)
Pyridaben	C19 H25 Cl N2 O S	GC	4	1.57×10^{-2}	−2.09	−76.5 (−78.1, −75)
trans-Allethrin	Cl9 H26 O3	GC	3	4.20×10^{-4}	−1.81	−71.5 (−72.3, −70.7)
PFAS						
6-H-Perfluorohexanoic acid	C6 H2 F10 O2	LC, −	3	6.54×10^{-3}	−9.86	−99.9 (−106, −93.7)
Perfluorobutane sulfonate (PFBS)	C4 H F9 O3 S	LC, −	1	7.67×10^{-3}	−13.21	−100 (−108, −91.4)

Identification or Putative Identification[a]	Formula	Analytical Method	Level	*p* value	Fold Change	% difference (95% CI)
Phthalates						
Diisobutyl phthalate	Cl6 H22 O4	GC	1	2.43×10^{-2}	−7.52	−99.5 (−105, −93.5)
Diisodecyl phthalate	C28 H46 O4	LC, −	3	1.13×10^{-2}	−1.45	−63.5 (−64.5, −62.5)
Dimethyl phthalate	ClO H10 O4	GC	1	6.10×10^{-4}	−2.89	−86.5 (−87.9, −85.2)
Plasticizers						
Heptyl 4-methylbenzenesulfonate	C14 H22 O3 S	LC, −	3	9.84×10^{-3}	−9.77	−99.9 (−106, −93.3)
Methylphthalic anhydride	C9 H6 O3	LC, −	3	1.17×10^{-4}	−10.71	−99.9 (−104, −95.7)
No Tentative Identification						
m/z 593.70459, 5.865 min		LC, +	5	$3.92 \times 10^{-}$	−2.31	−79.8 (−80.8, −78.8)
m/z 212.99615, 4.17 min		LC, −	5	3.96×10^{-3}	−1.07	−52.3 (−52.9, −51.7)
m/z 239.05997, 7.016 min		LC, −	5	1.46×10^{-3}	−1.16	−55.2 (−55.8, −54.6)
m/z 86.03174, 11.135 min		GC	5	3.95×10^{-3}	−1.22	−57.2 (−57.9, −56.5)
m/z 54.04641, 11.622 min		GC	5	2.37×10^{-2}	−1.57	−66.4 (−67.6, −65.2)
m/z 110.07266, 17.921 min		GC	5	1.39×10^{-2}	−1.67	−68.6 (−69.8, −67.4)
m/z 97.06492, 29.351 min		GC	5	2.70×10^{-2}	−1.06	−52.1 (−52.9, −51.2)
m/z 196.08382, 30.011 min		GC	5	1.39×10^{-3}	−1.18	−55.7 (−56.3, −55.1)
m/z 196.08862, 31.245 min		GC	5	4.12×10^{-4}	−1.22	−57.2 (−57.7, −56.6)
m/z 235.14832, 34.496 min		GC	5	2.50×10^{-2}	−2.32	−80 (−81.8, −78.1)
m/z 106.06521, 35.393 min		GC	5	1.44×10^{-2}	−1.00	−50 (−50.7, −49.3)
m/z 140.08316, 36.495 min		GC	5	1.79×10^{-3}	−1.09	−53 (−53.6, −52.5)
m/z 279.13818, 38.322 min		GC	5	1.24×10^{-2}	−1.56	−66.1 (−67.2, −65)
m/z 139.07538, 39.273 min		GC	5	2.23×10^{-2}	−2.61	−83.6 (−85.6, −81.6)
m/z 170.10883, 39.398 min		GC	5	2.07×10^{-2}	−1.01	−50.2 (−51, −49.5)
m/z 106.53482, 39.456 min		GC	5	1.61×10^{-2}	−1.90	−73.2 (−74.6, −71.8)
m/z 184.11252, 43.172 min		GC	5	1.29×10^{-2}	−1.74	−70.1 (−71.3, −68.9)
m/z 222.13596, 43.552 min		GC	5	2.52×10^{-2}	−1.00	−50 (−50.8, −49.2)
m/z 161.05984, 43.811 min		GC	5	2.38×10^{-2}	−1.33	−60.1 (−61.2, −59.1)
m/z 259.14841, 43.89 min		GC	5	2.02×10^{-2}	−1.53	−65.4 (−66.5, −64.2)

J Expo Sci Environ Epidemiol. Author manuscript; available in PMC 2024 June 19.

Identification or Putative Identification[a]	Formula	Analytical Method	Level	*p* value	Fold Change	% difference (95% CI)
m/z 135.49243, 8.339 min		GC	5	1.14×10^{-2}	−1.06	−52 (−52.7, −51.3)
m/z 152.15585, 9.584 min		GC	5	8.52×10^{-3}	−2.21	−78.3 (−79.8, −76.9)

[a] Relative abundance declined by at least 50% and the p value was less than the 20% FDR threshold.